

Conference Report

Nucleosynthesis Predictions and High-Precision Deuterium Measurements

Signe Riemer-Sørensen * and Espen Sem Jenssen

Institute of Theoretical Astrophysics, The University of Oslo, Boks 1072 Blindern, NO-0316 Oslo, Norway; EspenJenssen@hotmail.com

* Correspondence: signe.riemer-sorensen@astro.uio.no

Academic Editors: Mariusz P. Dąbrowski, Manuel Krämer and Vincenzo Salzano

Received: 9 January 2017; Accepted: 3 May 2017; Published: 9 May 2017

Abstract: Two new high-precision measurements of the deuterium abundance from absorbers along the line of sight to the quasar PKS1937–1009 were presented. The absorbers have lower neutral hydrogen column densities ($N(\text{HI}) \approx 18 \text{ cm}^{-2}$) than for previous high-precision measurements, boding well for further extensions of the sample due to the plentitude of low column density absorbers. The total high-precision sample now consists of 12 measurements with a weighted average deuterium abundance of $\text{D}/\text{H} = 2.55 \pm 0.02 \times 10^{-5}$. The sample does not favour a dipole similar to the one detected for the fine structure constant. The increased precision also calls for improved nucleosynthesis predictions. For that purpose we have updated the public AlterBBN code including new reactions, updated nuclear reaction rates, and the possibility of adding new physics such as dark matter. The standard Big Bang Nucleosynthesis prediction of $\text{D}/\text{H} = 2.456 \pm 0.057 \times 10^{-5}$ is consistent with the observed value within 1.7 standard deviations.

Keywords: (cosmology:) cosmological parameters; (cosmology:) primordial nucleosynthesis; (galaxies:) quasars: absorption lines; nuclear reactions; nucleosynthesis; abundances

1. Introduction

Consisting only of a proton and a neutron, deuterium is the simplest element, and consequently it was the first one to form in the early universe. The nucleosynthesis of the light elements such as deuterium, helium and lithium took place during the first few minutes after Big Bang when the universe was still opaque, and today we can only probe the conditions indirectly through the resulting abundances. This requires high precision measurements combined with reliable predictions for the abundances. In Section 2 we provide a short overview of the nucleosynthesis, before we present new high precision measurements of the deuterium abundance in Section 3 and a new code for performing predictions in Section 4.

2. Background

In order to form bound nuclei it is necessary to have free neutrons and protons with temperatures below their binding energy. The decoupling of the weak interaction and consequently the appearance of free neutrons and protons happens already around one second after Big Bang, but the binding energy of deuterium is as low as 2.2 MeV. Since deuterium is the simplest element you can form, the consequence of the low binding energy is a delay of the nucleosynthesis until 2–3 min after Big Bang. Meanwhile the free neutrons decay, altering the final abundances of deuterium and helium.

During Big Bang Nucleosynthesis only light elements are formed because helium is very strongly bound (binding energy of 28.3 MeV) and there exist no stable nucleus with five nucleons. This means you cannot fuse helium and neutrons/protons into heavier elements, providing a severe bottleneck for

the formation of heavier elements. Due to the decay of free neutrons, only the ones that become bound in nuclei survive. Most of the produced deuterium is converted to helium, leaving only of the order of 10^{-5} deuterium nuclei per hydrogen nuclei.

The formation of the light elements is sensitive to the expansion rate (temperature) and timing of the events e.g., decoupling, and consequently the abundances of the light elements can probe the conditions during the nucleosynthesis.

3. Observational Deuterium Measurements

Neutral deuterium has absorption features similar to the Lyman series of hydrogen, but with a $82 \text{ km} \cdot \text{s}^{-1}$ off-set because of the heavier nucleus. Consequently we can measure the “fingerprint” of deuterium caused by absorption in gas clouds along the line of sight to distant bright sources such as quasars. However, due to the fairly small off-set and low abundance of deuterium relative to hydrogen ($D/H = 10^{-5}$), high resolution spectra ($R \approx 45000$) with very good signal to noise are required. Given that there are no significant astrophysical sources of deuterium production [1,2] and the destruction rate in stars is low at the relevant redshifts and metallicities [3,4], medium-to-high redshift measurements will be very close to the primordial value.

Here we present two new high precision measurements along the line of sight to the quasar PKS1937–101. The absorber at $z_{\text{abs}} = 3.572$ was previously analysed by Tytler et al. [5], Burles and Tytler [6], and the $z_{\text{abs}} = 3.256$ absorber was analysed by Crighton et al. [7]. New spectra of the quasar have become available in the form of 63.4 ks exposures from the High Resolution Echelle Spectrometer (HIRES) at the Keck Telescope and 32.4 ks from the Ultraviolet and Visual Echelle Spectrograph (UVES) at the Very Large Telescope (VLT). A root-mean-square weighted stacking of the new spectra is shown in Figure 1. The spectra are reduced and normalised following standard procedures and the relevant atomic transitions are fitted with a model consisting of several Voigt-profiles that represent the individual sub-components of the absorbers. Each sub-component is characterised by a redshift, a column density, a temperature and a turbulent broadening. In addition, we allow for uncertainties in the continuum normalisation and calibration of the spectra. The details of the spectra and their analyses can be found in Riemer-Sørensen et al. [8,9], and here we only discuss the results.

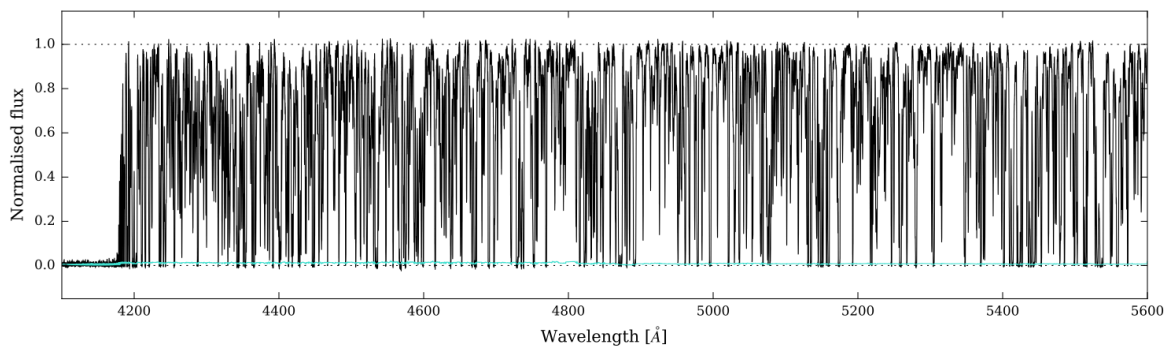


Figure 1. The normalised flux spectrum of PKS1937–101 (weighted stacking of all exposures for illustration only). The Lyman α of the $z_{\text{abs}} = 3.256$ absorber lies at 5171.7 \AA and the Lyman Limit at 3877.2 \AA (outside the spectrum). For the $z_{\text{abs}} = 3.572$ the Lyman α is found at 5555.7 \AA and the Lyman Limit at 4165.1 \AA .

3.1. Deuterium in the $z_{\text{abs}} = 3.256$ Absorber

We fit the absorption with Voigt profiles using VPFIT [10] to obtain the gas cloud characteristics including the deuterium and hydrogen abundances. We find a deuterium abundance of $D/H = 2.45 \pm 0.28 \times 10^{-5}$ to be compared with the previous measurement of $D/H = 1.6 \pm 0.30 \times 10^{-5}$ [7]. If naively interpreted as a statistical fluctuation this corresponds to a 3σ difference. However, it originates in a systematic model difference, which is hard to quantify. The measurement from the new spectra

is not more precise despite the increased signal-to-noise ratio, but we believe it to be more robust, as the better data allow us to resolve the internal structure of the absorber better. This is illustrated in Figure 2. The best fit model is consistent between the UVES and HIRES spectra.

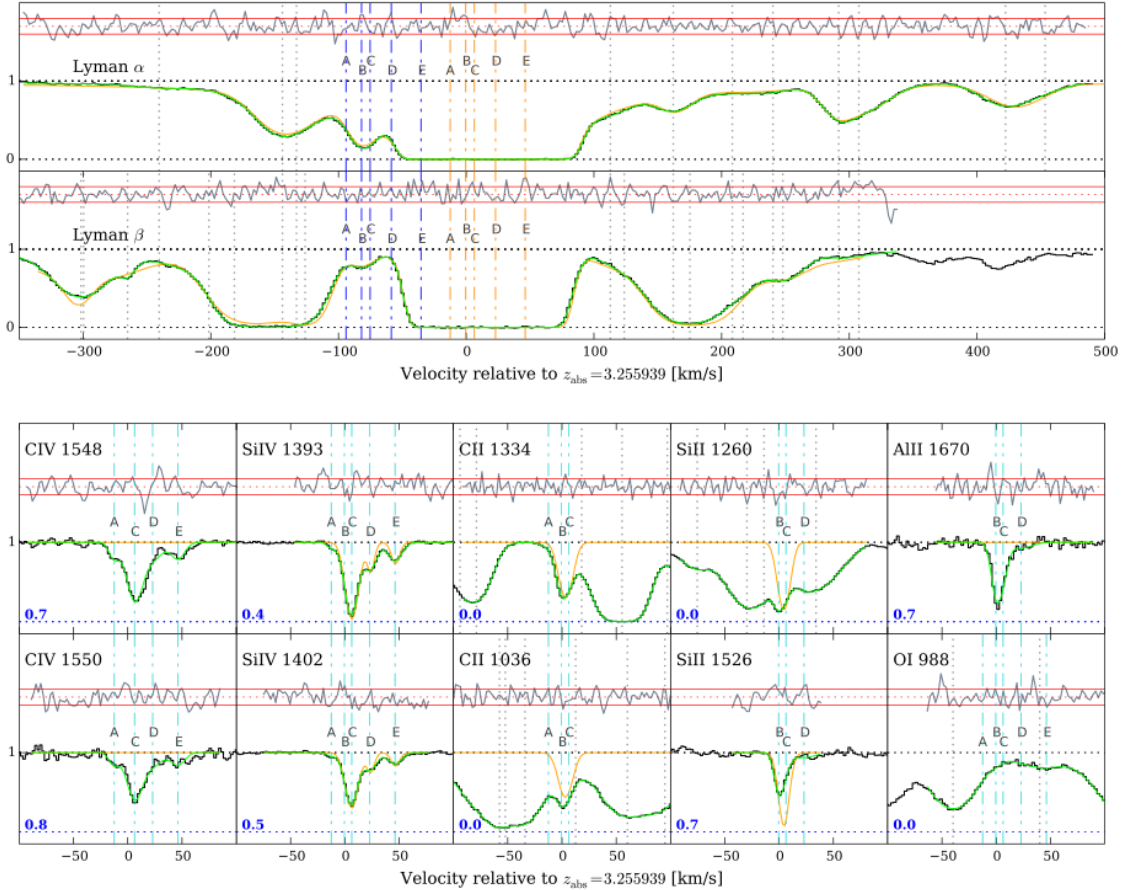


Figure 2. The normalised stacked flux spectrum (thick black) of the $z_{\text{abs}} = 3.256$ absorber, and the best fit model (green), as well as the normalised fit residuals (above each fit). The stacked spectrum is only used for visualisation, as the model fitting is always performed on the individual spectra simultaneously. The fitted velocity components are marked by vertical dot-dashed lines denoted by A to F (HI in orange, DI in blue, metals in cyan), and interloping HI lines are shown as vertical dotted lines (light grey). It is seen that the structure of the absorber is more complicated than the old model from Crighton et al. [7] (orange), which has a significant impact on the final result. Figure from [8].

3.2. Deuterium in the $z_{\text{abs}} = 3.572$ Absorber

For the high redshift absorber we find a ratio of $D/H = 2.62 \pm 0.03 \times 10^{-5}$ to be compared with the previous measurement of $D/H = 3.3 \pm 0.3 \times 10^{-5}$ [6]. In contrast to Burles and Tytler [6] we include the heavy element transitions in the model fitting, resulting in a more complicated substructure for the absorber as shown in Figure 3. The interesting point here is the very high precision we obtain, even though the hydrogen column density of $\log(N(\text{HI})) = 17.9$ is lower than for previous similar high-precision measurements [11]. This is important for future measurements because the neutral hydrogen column density distribution in quasar absorption systems is a steep power law, with lower column density systems being more common. A statistically large sample of measurements is therefore feasible and at the same time strictly necessary in order to reveal a plateau of primordial values as a function of, e.g., metallicity. Despite the complexity of the absorber, the very high precision on the D/H ratio is obtained due to a combination of (1) very high signal to noise ratio in the

spectra; (2) fitting 9 Lyman transitions for which the oscillator strengths span more than two orders of magnitude; and (3) the presence of several heavy element species that allow us to constrain the velocity structure of the system.

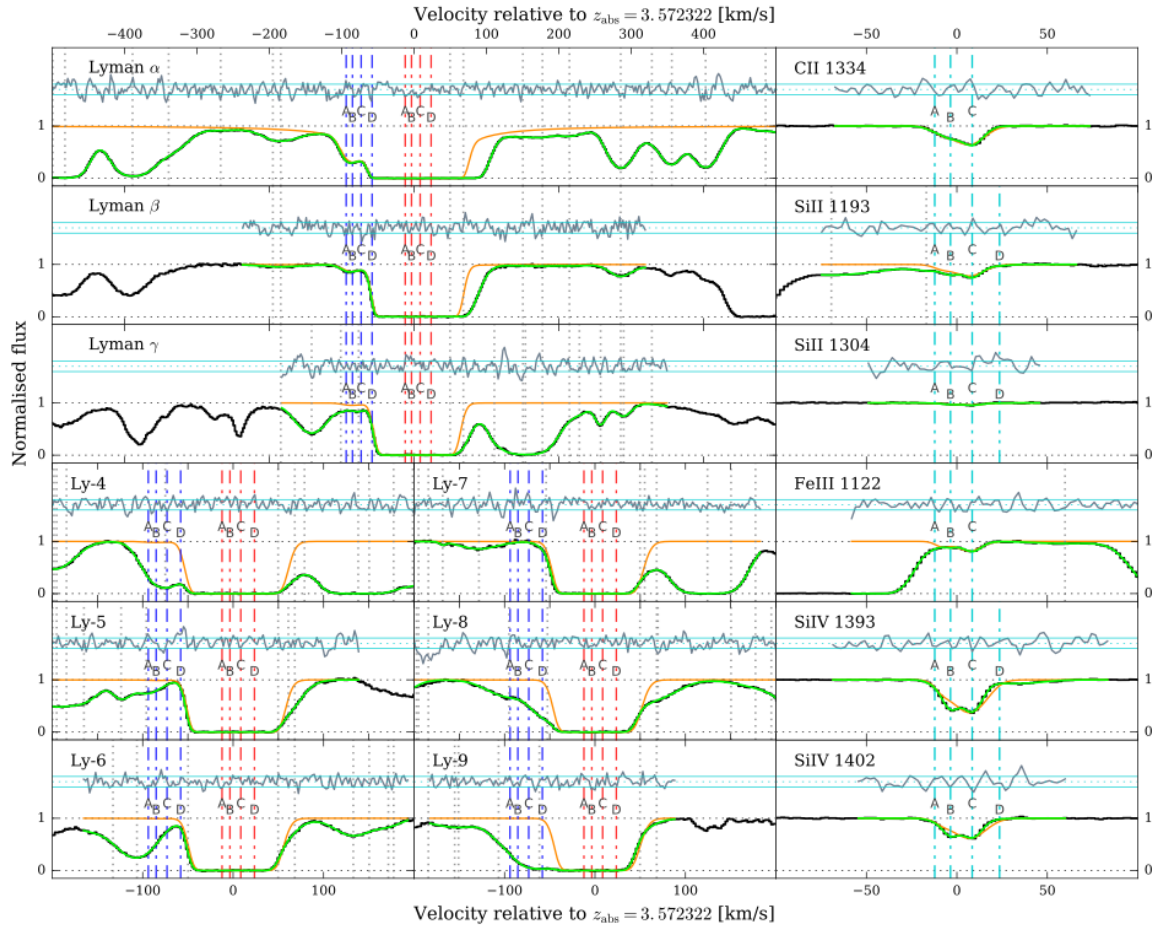


Figure 3. The normalised stacked flux spectrum (thick black) of the $z_{\text{abs}} = 3.572$ absorber, and the best fit model (green), as well as the normalised fit residuals (above each fit). The stacked spectrum is only used for visualisation, as the model fitting is always performed on the individual spectra simultaneously. The fitted velocity components are marked by vertical dot-dashed lines denoted by A to D (HI in red, DI i in blue, metals in cyan), and interloping HI lines are shown as vertical dotted lines (light grey). The model from Tytler et al. [5] (without blends) is over-plotted in orange, illustrating the difference between the derived model structures, particularly for the metals. Figure from [9].

3.3. Deuterium Measurement Sample

For standard Big Bang Nucleosynthesis the inferred value of the primordial deuterium abundance can be used to infer the baryon density of the universe, Ω_b . Table 1 provide a list of current measurements, for which the weighted average is $100\Omega_b h^2 = 2.17 \pm 0.024$ which deviates by 1.9σ from the value of 2.225 ± 0.016 inferred from the measurements of the cosmic microwave background [12]. We consider the two results to be consistent.

We find no correlations between deuterium abundance and redshift, metallicity or hydrogen column density (as tentatively claimed by Cooke et al. [13]). Neither do we find any evidence for a dipole in the deuterium measurements [9]. Such a dipole would be expected if there were variations in fundamental constants like the fine structure constant, the hadronic masses or binding energies [14]. As an example we consider a dipole with the same direction as the potential dipole in the fine structure

constant [15,16], for which the preferred slopes are close to zero with uncertainties larger than the preferred value and consequently consistent both with a small dipole and with no dipole.

Table 1. The sample of D I/H I measurements from Riemer-Sørensen et al. [9]

Reference	Absorption Redshift	$\log(N(\text{H I}))$	[X/H]	D I/H I [$\times 10^{-5}$]	$100 \Omega_b h^2$
Burles and Tytler [6]	2.504	17.4 ± 0.07	−2.55 Si	4.00 ± 0.70	1.66 ± 0.18
Pettini and Bowen [17]	2.076	20.4 ± 0.15	−2.23 Si	1.65 ± 0.35	2.82 ± 0.36
Kirkman et al. [18]	2.426	19.7 ± 0.04	−2.79 O	2.43 ± 0.35	2.24 ± 0.20
Fumagalli et al. [19]	3.411	18.0 ± 0.05	−4.20 Si	2.04 ± 0.61	2.49 ± 0.05
Noterdaeme et al. [20] ¹	2.621	20.5 ± 0.10	−1.99 O	2.80 ± 0.80	2.05 ± 0.35
Cooke et al. [11], Pettini and Cooke [21]	3.050	20.392 ± 0.003	−1.92 O	2.51 ± 0.05	2.19 ± 0.02
Cooke et al. [11], O’Meara et al. [22]	2.537	19.4 ± 0.01	−1.77 O	2.58 ± 0.15	2.16 ± 0.04
Cooke et al. [11], Pettini et al. [23]	2.618	20.3 ± 0.01	−2.40 O	2.53 ± 0.10	2.18 ± 0.03
Cooke et al. [11]	3.067	20.5 ± 0.01	−2.33 O	2.58 ± 0.07	2.16 ± 0.03
Cooke et al. [11], O’Meara et al. [24]	2.702	20.7 ± 0.05	−1.55 O	2.40 ± 0.14	2.25 ± 0.03
Riemer-Sørensen et al. [8]	3.255	18.1 ± 0.03	−1.87 O	2.45 ± 0.28	2.23 ± 0.16
Balashev et al. [25] ¹	2.437	19.98 ± 0.01	−2.04 O	1.97 ± 0.33	2.54 ± 0.26
Cooke et al. [13]	2.853	20.34 ± 0.04	−2.08 O	2.55 ± 0.03	2.17 ± 0.03
Riemer-Sørensen et al. [9]	3.572	17.925 ± 0.006	−2.26 O	2.62 ± 0.05	2.14 ± 0.03
Weighted average ¹	—	—	—	2.55 ± 0.02	2.17 ± 0.02
Unweighted average ¹	—	—	—	2.53 ± 0.16	2.18 ± 0.08
Planck Collaboration et al. [12]	—	—	—	2.45 ± 0.05	2.225 ± 0.016

In order to convert between D I/H I and $\Omega_b h^2$ we assume standard nucleosynthesis and use the nuclear rates from Coc et al. [26].¹ The Balashev et al. [25] and Noterdaeme et al. [20] measurements are excluded from the average because they are derived under the assumption of constant O I/H I across all components, which may not be an appropriate assumption for a high precision measurement.

4. Predictions from Nucleosynthesis

The improved observational precision calls for nucleosynthesis predictions with similar accuracy. We have updated and expanded the existing AlterBBN code with nuclear rates and non-standard physics options. AlterBBN is a publicly available C code for evaluating abundances [27], which is based on the Wagoner code [28] and similar to NUC123 ([29], also known as the Kawano code) and PArthENoPE [30]¹. AlterBBN can be run as an independent code or included in multi-parameter analyses using e.g., CosmoMC² or Montepython³. Until the improvements described here are implemented in the official version of AlterBBN, the code and further details can be obtained from github.com/espensem/AlterBBN.

AlterBBN evaluates the light element abundances as a function of time during the Big Bang Nucleosynthesis (BBN). It starts from a thermodynamic equilibrium, whereafter the weak interaction and the neutrinos decouple, leading to the decay of free neutrons. Eventually the electrons and positrons will decouple and annihilate, which will reheat the photons (and any other particles with an electromagnetic coupling). Until the photon temperature has dropped below the binding energy of deuterium, the protons and neutrons cannot form any deuterium.

The resulting abundances depend on the nuclear reaction rates and the timing/expansion in the early universe. Without any non-standard physics, the baryon to photon ratio is the only free parameter in BBN. Since it can be determined very precisely from the cosmic microwave background [12], the main uncertainty in the predictions comes from the nuclear reaction rates.

4.1. Updating Nuclear Reaction Rates

We have extended the nuclear network in AlterBBN from 88 to 100 reactions, and updated six important rates with new theoretical/experimental determinations [26]. The resulting helium

¹ PArthENoPE is also publicly available, but it requires expensive fortran libraries to compile

² <http://cosmologist.info/cosmomc>

³ <http://baudren.github.io/montepython.html>

and hydrogen-3 abundances are relatively unaffected by these changes, but D/H change by 4.5%, and the uncertainty double. Lithium-7 and beryllium-7 increase by 18% thereby worsening the lithium problem.

An example of the updated rates is the formation of helium-3 via $d(p,\gamma)^3\text{He}$. For this rate there is only very scarce experimental data at the relevant energy range [31]. Instead the rates have been determined theoretically or from fitting various polynomials or theoretical models to an extended energy range and extrapolating to the range of interest. The newest theoretical calculation by Marcucci et al. [32] is inconsistent with the experimental rate measured around 0.1 MeV. To reconcile the discrepancy Coc et al. [26] rescaled the theoretical model from Viviani et al. [33], Marcucci et al. [34] to the experimental rates for the full range of 0.002–2 MeV. Using AlterBBN with the theoretically determined rate from [32] leads to $D/H = 2.49 \pm 0.03 \pm 0.03 \times 10^{-5}$ (the two errors are due to nuclear rate uncertainties and uncertainties in the baryon density, respectively) while the experimental rescaling from [26] leads to $D/H = 2.45 \pm 0.057 \times 10^{-5}$. The two results deviate by approximately 1σ .

Another option is to use the experimental data directly (as in e.g., [35,36])⁴, which will further increase the deviation between the various predictions from AlterBBN. At this point we do not want to advocate one choice over another, but simply want to emphasise that the choice of rates matters, and unless the specific choice is discussed in the context of each result (which is usually not the case (e.g., [8,11,25])), this deviation between rates should be included as a systematic uncertainty. Better experimental determination of the rates at BBN energies will solve the issue.

4.2. Implementing New Physics

Non-standard physics such as extra relativistic species, modified gravity or lepton asymmetry may change the expansion rate in the early universe or the order of the events governing the nucleosynthesis [37–39]. These effects could potentially originate in production/destruction of dark matter or neutrino-like species. At present and, likely for the foreseeable future, BBN provides the only window to a universal lepton asymmetry. The most obvious way to generate lepton asymmetry is via additional neutrino species

We have updated AlterBBN with the possibility of adding the presence of equivalent neutrinos (non-interacting relativistic species) and Weakly Interacting Massive Particles (WIMPs) during the nucleosynthesis. The WIMPs are generic and their effect is purely determined by their mass, the number of internal degrees of freedom, their nature (fermion or boson) as well as any coupling to the standard model particles. The WIMPs can be either electromagnetically coupled or coupled to neutrinos (standard model neutrinos and any equivalent species) (following [38,39]). They are not required to provide 100% of the dark matter but could be a subcomponent. We consider four types of WIMPs: (1) Real scalars that are self-conjugate and have one degree of freedom; (2) Complex scalars that have two degrees of freedom; (3) Majorana fermions which are self-conjugate and have two degrees of freedom; and (4) Dirac fermions with four degrees of freedom.

The presence of such non-standard model particles will alter the expansion rate because they contribute to the total energy density. They might also increase the temperature of photons or neutrinos due to annihilation, and by mimicking neutrinos, they might change the inferred number of relativistic species often parametrised as a change in the number of neutrino species $N_{\text{eff}} = 3.046 + \Delta N_\nu$ where ΔN_ν is the equivalent number of neutrinos that would provide the same effect (e.g., [40,41]). The relativistic particles contribute to the radiation energy density so that $\rho_{\text{rad}} \rightarrow \rho'_{\text{rad}} = \rho_{\text{rad}} + \Delta N_\nu \rho_\nu$. Combining with the Friedman equation [42] we can relate the expansion factor directly to N_{eff} as

$$\frac{H'}{H} = \left(\frac{\rho'_{\text{rad}}}{\rho_{\text{rad}}} \right)^{1/2} = \left(1 + \frac{7\Delta N_\nu}{43} \right)^{1/2} \quad (1)$$

⁴ To be implemented in the next version of AlterBBN

where H'/H is the relative expansion rate with and without the extra species. Similarly, lepton asymmetry can be parametrised in terms of N_{eff} (see e.g., [37]), and an increase in entropy (e.g., from decaying dark matter) will affect the number of degrees of freedom, which can also be expressed as a change in N_{eff} .

In Figure 4 we show the probability contours for simultaneously varying the baryon density ($\eta = n_b/n_\gamma$) and the additional number of neutrinos for otherwise standard BBN and comparing to observational constraints on D I/H I and ^4He . As seen the constraints from BBN alone are consistent with those from the *Planck Surveyor* and of comparable precision. The combined D I/H I and ^4He constraint on ΔN_ν is $\Delta N_\nu = 0.06^{+0.27}_{-0.36}$.

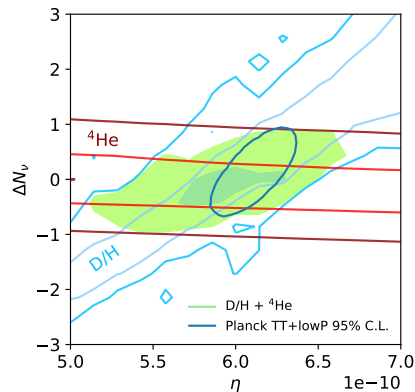


Figure 4. Constraints in the $\eta - \Delta N_\nu$ plane (68% and 98% C.L.) from observations of D/H (light blue lines, from [9]), ^4He (red lines, from [43]), and combined (green shade). We also show the 95% contours for the *Planck Surveyor* for comparison (dark blue, from TT + LowP in [12]).

Including WIMPs will change the radiation and/or matter energy density and pressure directly, as well as possible changes in the entropy and lepton asymmetry depending on the specific properties. The expansion rate governs the particle number densities and consequently the interaction rates for nucleosynthesis. Figure 5 illustrate the changes of the D/H ratio when including WIMPs in the mass range from 0.01 to 100 MeV (heavier or lighter WIMPs will provide linear extensions of the abundance in Figure 5 as they decouple completely before/after the nucleosynthesis). The results are compared to those of [38,39]. The deviations are due to different choices of nuclear rates (e.g., the [38,39] results are based on the theoretical calculation of $d(p,\gamma)^3\text{He}$ from [33] while we have used the experimentally rescaled rate from [26]). Comparing to the observational constraints, we see that for electromagnetically coupled WIMPs we can exclude masses below 10 MeV and for neutrino coupled WIMPs only masses around 10 MeV are allowed.

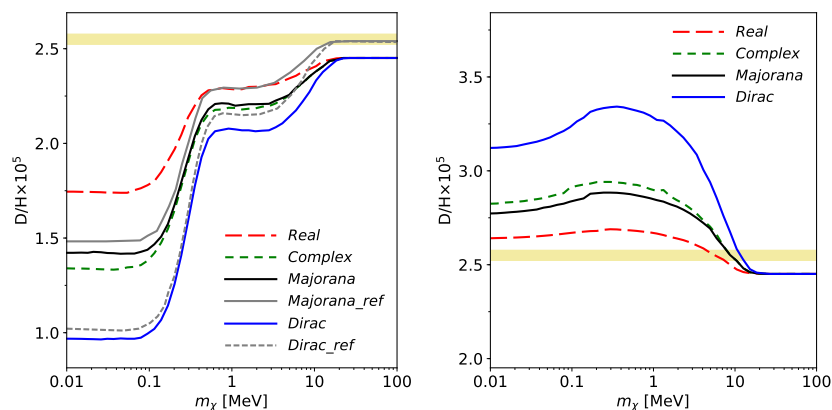


Figure 5. The deuterium abundance as a function of Weakly Interacting Massive Particles (WIMP) mass if the WIMP is a real scalar (dashed red), a complex scalars (dotted green), Majorana fermion (solid black), Dirac fermion (solid blue). The left plot is for electromagnetically coupled WIMPs (coupling to electrons or photons) and the right plot is for neutrino coupling. The grey lines are for comparison to [38,39]. The deviations are due to different choices of nuclear rates. The yellow horizontal bands are the observed ratio of D/H [8]. Figure from [44].

Neither non-standard physics nor the new rates alleviate the Lithium problem.

5. Summary

We have presented new high precision measurement of the deuterium to hydrogen ratio from low column density absorbers ($N(\text{H I}) = 17.9$ and 18.1 cm^{-2}) along the line of sight to the quasar PKS1937–101. This is important for future measurements because the neutral hydrogen column density distribution in quasar absorption systems is a steep power law, with lower column density systems being more common. A statistically large sample of measurements is therefore feasible.

With the acquired precision on the observational measurements, it is timely to similarly improve the theoretical predictions from Big Bang nucleosynthesis. We have updated the publicly available code, AlterBBN, with new reaction rates and non-standard physics. It is clear that the choice between theoretical and measured rates at relevant energies leads to different results, providing a source of systematic uncertainty which is often neglected.

Supplementary Materials: The updates of AlterBBN is available here github.com/espensem/AlterBBN and will be included in the next official and distributed release of AlterBBN.

Acknowledgments: The authors would like to thank the anonymous referees for constructive comments and suggestions.

Author Contributions: All the authors equally contributed to this work.

Conflicts of Interest: The authors declare no conflict of interest.

References

1. Epstein, R.I.; Lattimer, J.M.; Schramm, D.N. The origin of deuterium. *Nature* **1976**, *263*, 198–202.
2. Prodanović, T.; Fields, B.D. On Nonprimordial Deuterium Production by Accelerated Particles. *Astrophys. J.* **2003**, *597*, 48.
3. Romano, D.; Tosi, M.; Chiappini, C.; Matteucci, F. Deuterium astration in the local disc and beyond. *Mon. Not. R. Astron. Soc.* **2006**, *369*, 295–304.
4. Dvorkin, I.; Vangioni, E.; Silk, J.; Petitjean, P.; Olive, K.A. Evolution of dispersion in the cosmic deuterium abundance. *Mon. Not. R. Astron. Soc. Lett.* **2016**, *458*, L104–L108.
5. Tytler, D.; Fan, X.M.; Burles, S. Cosmological baryon density derived from the deuterium abundance at redshift $z = 3.57$. *Nature* **1996**, *381*, 207–209.
6. Burles, S.; Tytler, D. The Deuterium Abundance toward Q1937-1009. *Astrophys. J.* **1998**, *499*, 699.

7. Crighton, N.H.M.; Webb, J.K.; Ortiz-Gil, A.; Fernández-Soto, A. Deuterium/hydrogen in a new Lyman limit absorption system at $z = 3.256$ towards PKS1937-1009. *Mon. Not. R. Astron. Soc.* **2004**, *355*, 1042–1052.
8. Riemer-Sørensen, S.; Webb, J.K.; Crighton, N.; Dumont, V.; Ali, K.; Kotuš, S.; Bainbridge, M.; Murphy, M.T.; Carswell, R. A robust deuterium abundance; re-measurement of the $z = 3.256$ absorption system towards the quasar PKS 1937-101. *Mon. Not. R. Astron. Soc.* **2015**, *447*, 2925–2936.
9. Riemer-Sørensen, S.; Kotuš, S.; Webb, J.K.; Ali, K.; Dumont, V.; Murphy, M.T.; Carswell, R. A robust deuterium abundance; re-measurement of the $z = 3.256$ absorption system towards the quasar PKS 1937-101. *Mon. Not. R. Astron. Soc.* **2017**, accepted.
10. Carswell, R.F.; Webb, J.K. *VPFIT: Voigt Profile Fitting Program*; Astrophysics Source Code Library: College Park, MD, USA, 2014.
11. Cooke, R.J.; Pettini, M.; Jorgenson, R.A.; Murphy, M.T.; Steidel, C.C. Precision Measures of the Primordial Abundance of Deuterium. *Astrophys. J.* **2014**, *781*, 31.
12. Planck Collaboration; Ade, P.A.R.; Aghanim, N.; Arnaud, M.; Ashdown, M.; Aumont, J.; Baccigalupi, C.; Banday, A.J.; Barreiro, R.B.; Bartlett, J.G.; et al. Planck 2015 results XIII. Cosmological parameters. *Astron. Astrophys.* **2016**, *594*, A13.
13. Cooke, R.J.; Pettini, M.; Nollett, K.M.; Jorgenson, R. The Primordial Deuterium Abundance of the Most Metal-poor Damped Lyman- α System. *Astrophys. J.* **2016**, *830*, 148.
14. Berengut, J.C.; Flambaum, V.V.; King, J.A.; Curran, S.J.; Webb, J.K. Is there further evidence for spatial variation of fundamental constants? *Phys. Rev. D* **2011**, *83*, 123506.
15. Webb, J.K.; King, J.A.; Murphy, M.T.; Flambaum, V.V.; Carswell, R.F.; Bainbridge, M.B. Indications of a Spatial Variation of the Fine Structure Constant. *Phys. Rev. Lett.* **2011**, *107*, 191101.
16. King, J.A.; Webb, J.K.; Murphy, M.T.; Flambaum, V.V.; Carswell, R.F.; Bainbridge, M.B.; Wilczynska, M.R.; Koch, F.E. Spatial variation in the fine-structure constant—New results from VLT/UVES. *Mon. Not. R. Astron. Soc.* **2012**, *422*, 3370–3414.
17. Pettini, M.; Bowen, D.V. A New Measurement of the Primordial Abundance of Deuterium: Toward Convergence with the Baryon Density from the Cosmic Microwave Background? *Astrophys. J.* **2001**, *560*, 41–48.
18. Kirkman, D.; Tytler, D.; Suzuki, N.; O’Meara, J.M.; Lubin, D. The Cosmological Baryon Density from the Deuterium-to-Hydrogen Ratio in QSO Absorption Systems: D/H toward Q1243+3047. *Astrophys. J. Suppl. Ser.* **2003**, *149*, 1–28.
19. Fumagalli, M.; O’Meara, J.M.; Prochaska, J.X. Detection of Pristine Gas Two Billion Years After the Big Bang. *Science* **2011**, *334*, 1245–1249.
20. Noterdaeme, P.; López, S.; Dumont, V.; Ledoux, C.; Molaro, P.; Petitjean, P. Deuterium at high redshift. Primordial abundance in the $z_{abs} = 2.621$ damped Ly- α system towards CTQ 247. *Astron. Astrophys.* **2012**, *542*, L33.
21. Pettini, M.; Cooke, R. A new, precise measurement of the primordial abundance of deuterium. *Mon. Not. R. Astron. Soc.* **2012**, *425*, 2477–2486.
22. O’Meara, J.M.; Tytler, D.; Kirkman, D.; Suzuki, N.; Prochaska, J.X.; Lubin, D.; Wolfe, A.M. The Deuterium to Hydrogen Abundance Ratio toward a Fourth QSO: HS 0105+1619. *Astrophys. J.* **2001**, *552*, 718–730.
23. Pettini, M.; Zych, B.J.; Murphy, M.T.; Lewis, A.; Steidel, C.C. Deuterium abundance in the most metal-poor damped Lyman alpha system: Converging on $\Omega_b h^2$. *Mon. Not. R. Astron. Soc.* **2008**, *391*, 1499–1510.
24. O’Meara, J.M.; Burles, S.; Prochaska, J.X.; Prochter, G.E.; Bernstein, R.A.; Burgess, K.M. The Deuterium-to-Hydrogen Abundance Ratio toward the QSO SDSS J155810.16-003120.0. *Astrophys. J. Lett.* **2006**, *649*, L61–L65.
25. Balashev, S.A.; Zavarygin, E.O.; Ivanchik, A.V.; Telikova, K.N.; Varshalovich, D.A. The primordial deuterium abundance: SubDLA system at $z_{abs} = 2.437$ towards the QSO J 1444+2919. *Mon. Not. R. Astron. Soc.* **2016**, *458*, 2188–2198.
26. Coc, A.; Petitjean, P.; Uzan, J.P.; Vangioni, E.; Descouvemont, P.; Iliadis, C.; Longland, R. New reaction rates for improved primordial D /H calculation and the cosmic evolution of deuterium. *Phys. Rev. D* **2015**, *92*, 123526.
27. Arbey, A. AlterBBN: A program for calculating the BBN abundances of the elements in alternative cosmologies. *Comput. Phys. Commun.* **2012**, *183*, 1822–1831.
28. Wagoner, R.V. Synthesis of the Elements Within Objects Exploding from Very High Temperatures. *Astrophys. J. Suppl. Ser.* **1969**, *18*, 247.

29. Kawano, L. *Let's Go: Early Universe. 2. Primordial Nucleosynthesis: The Computer Way*; NASA Technical Reports Server (NTRS): Hampton, VA, USA, 1992.
30. Pisanti, O.; Cirillo, A.; Esposito, S.; Iocco, F.; Mangano, G.; Miele, G.; Serpico, P.D. PARthENoPE: Public algorithm evaluating the nucleosynthesis of primordial elements. *Comput. Phys. Commun.* **2008**, *178*, 956–971.
31. Ma, L.; Karwowski, H.J.; Brune, C.R.; Ayer, Z.; Black, T.C.; Blackmon, J.C.; Ludwig, E.J.; Viviani, M.; Kievsky, A.; Schiavilla, R. Measurements of $^1\text{H}(d \rightarrow, fl)^3\text{He}$ and $^2\text{H}(p \rightarrow, fl)^3\text{He}$ at very low energies. *Phys. Rev. C* **1997**, *55*, 588–596.
32. Marcucci, L.E.; Mangano, G.; Kievsky, A.; Viviani, M. Implication of the Proton-Deuteron Radiative Capture for Big Bang Nucleosynthesis. *Phys. Rev. Lett.* **2016**, *116*, 102501.
33. Viviani, M.; Kievsky, A.; Marcucci, L.E.; Rosati, S.; Schiavilla, R. Photodisintegration and electrodisintegration of ^3He at threshold and pd radiative capture. *Phys. Rev. C* **2000**, *61*, 064001.
34. Marcucci, L.E.; Viviani, M.; Schiavilla, R.; Kievsky, A.; Rosati, S. Electromagnetic structure of $A = 2$ and 3 nuclei and the nuclear current operator. *Phys. Rev. C* **2005**, *72*, 014001.
35. Iocco, F.; Mangano, G.; Miele, G.; Pisanti, O.; Serpico, P.D. Primordial nucleosynthesis: From precision cosmology to fundamental physics. *Phys. Rep.* **2009**, *472*, 1–76.
36. Cyburt, R.H.; Fields, B.D.; Olive, K.A.; Yeh, T.H. Big bang nucleosynthesis: Present status. *Rev. Mod. Phys.* **2016**, *88*, 015004.
37. Steigman, G. Neutrinos and Big Bang Nucleosynthesis. *Adv. High Energy* **2012**, *2012*, 268321.
38. Nollett, K.M.; Steigman, G. BBN and the CMB constrain light, electromagnetically coupled WIMPs. *Phys. Rev. D* **2014**, *89*, 083508.
39. Nollett, K.M.; Steigman, G. BBN and the CMB constrain neutrino coupled light WIMPs. *Phys. Rev. D* **2015**, *91*, 083505.
40. Lesgourgues, J.; Pastor, S. Massive neutrinos and cosmology. *Phys. Rep.* **2006**, *429*, 307–379.
41. Riemer-Sørensen, S.; Parkinson, D.; Davis, T.M.; Blake, C. Simultaneous Constraints on the Number and Mass of Relativistic Species. *Astrophys. J.* **2013**, *763*, 89.
42. Friedmann, A. Über die Möglichkeit einer Welt mit konstanter negativer Krümmung des Raumes. *Z. Phys.* **1924**, *21*, 326–332.
43. Aver, E.; Olive, K.A.; Skillman, E.D. The effects of He I $\lambda 10830$ on helium abundance determinations. *J. Cosmol. Astropart. Phys.* **2015**, *7*, 011.
44. Jenssen, E.S. *New AlterBBN: A Code for Big Bang Nucleosynthesis with Light Dark Matter*. Master's Thesis, Institute of Theoretical Astrophysics, University of Oslo, Oslo, Norway, 2016.



© 2017 by the authors. Licensee MDPI, Basel, Switzerland. This article is an open access article distributed under the terms and conditions of the Creative Commons Attribution (CC BY) license (<http://creativecommons.org/licenses/by/4.0/>).